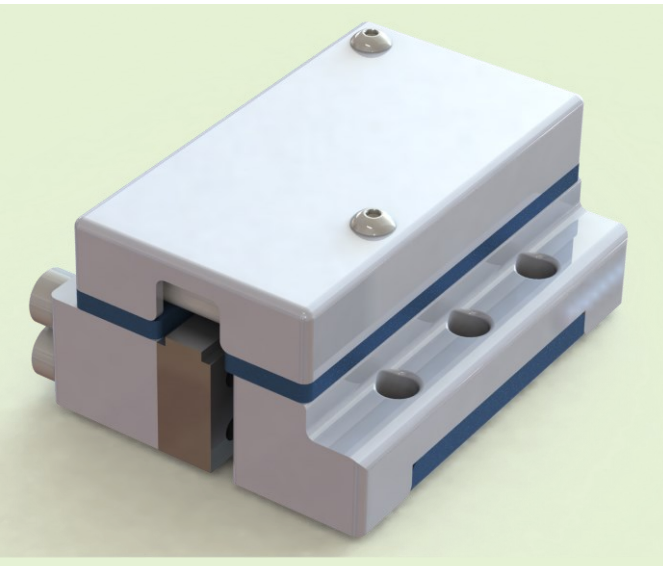


Smart Lacelock: A Shoelace Tensioning Device Motion Sensing

Md Rejwanul Haque, Md. Rafi Islam, Zahra Bassiri, Edward Sazonov, Dario Martelli and Xiangrong Shen

Abstract— Shoe-mounted wearable sensors may serve a variety of important purposes (activity recognition, energy expenditure estimation, etc.) by providing rich information about human locomotion. However, reliably attaching such sensors to shoes still remains a challenge. Further, pressure-sensing elements in such shoe sensor systems often suffer from poor durability due to the large dynamic load. This work presents a novel shoe-mounted sensor named Smart Lacelock, which takes the form of a common shoelace tensioning device (shoelace lock). With its unique form factor, the Smart Lacelock can be securely attached to the top of a shoe with minimal effort, enabling its embedded inertia measurement unit to provide reliable 3D motion measurement of the foot. Further, the Smart Lacelock incorporates a loadcell to measure the force applied by the shoelace, providing valuable information related to the ankle movement, foot/shoe shape change, and ground force. Design details of the device are presented, including the mechanical structure and electronic circuitry. The authors also conducted a 10participant human study, in which signals were recorded during free ankle swing, body weight shifting, sit-to-stand



Smart Lacelock Device

(STS), and overground walking. The results demonstrated the *Smart Lacelock*'s capability of providing consistent and observable responses to single contributing factors (ankle movement and foot loading) as well as complex movements with clearly defined events of interest (STS and walking). Such unique capability suggests that the *Smart Lacelock* may serve as an important source of human movement information to support related applications such as activity recognition and gait event detection.

Index Terms—locomotion sensing, Smart Lacelock, wearable sensors

I. INTRODUCTION

INERTIA measurement unit (IMU) is a special type of micro electro-mechanical system (MEMS) providing three-dimensional acceleration and angular velocity measurements. Commercial IMUs are becoming increasingly compact and affordable, enabling their ubiquitous application in portable electronic devices [1]–[6]. Benefiting from such technological advances, IMU-based wearable motion sensors have been developed to provide the 3D measurement of human

The manuscript is submitted on 15, January 2022.

This work was supported by the National Science Foundation under Grant 1734501.

Md Rejwanul Haque, Zahra Bassiri, Dario Martelli, and Xiangrong Shen are with the Department of Mechanical Engineering, The University of Alabama, Tuscaloosa, AL, USA.

(e-mail: mhaque2@crimson.ua.edu, zbassiri@crimson.ua.edu, dmartelli@eng.ua.edu, and xshen@eng.ua.edu)

Md Rafi Islam, and Edward Sazonov are with the Department of Electrical and Computer Engineering, The University of Alabama, Tuscaloosa. AL 35401 USA.

(e-mail: mislam24@crimson.ua.edu, and esazonov@eng.ua.edu).

movement, which displays multiple advantages over the traditional marker-based motion capture systems (e.g., lower cost and portability). However, reliably attaching wearable IMU sensors to different parts of the human body still remains a challenge. The traditional strap-based mounting method is inconvenient to use, and a strap-mounted sensor may shift its position during even mild human movement.

Presumably for the convenience of sensor attachment in daily use, the majority of existing wearable motion sensors on the commercial market are wrist-worn devices, including smart watches and wrist bands. Through the measured wrist movement, such sensors can potentially be used for physical activity monitoring and energy expenditure estimation. However, the performance of wrist sensors is less than satisfactory, largely due to the fact that the underlying wrist movement is a poor indicator of the user's full-body movement in locomotion.

As a promising alternative to wrist-worn sensors, footwear (shoe)-mounted wearable sensors have received increasing attention from researchers in both academia and industry.

Footwear is an irreplaceable part of modern human life, which acts as an interface between the ground and the wearer's foot and has direct involvement in full-body/lower-limb motion. While the primary purpose of footwear was to protect the feet [7], rich information (especially that related to human locomotion) can be obtained by monitoring its motion and its interaction with the environment. Attempts to obtain such information by integrating wearable sensors in footwear started in the 1990s, both in academic research and industrial products [8], and have become an increasingly popular area of research in recent years.

Footwear-based human locomotion monitor and various analysis systems have been proposed and applied both to healthy individuals and patients with neurological disorders [8]–[16]. Typically, footwear-based wearable sensor systems consist of pressure sensors for plantar pressure measurement and inertial sensors (accelerometer and/or gyroscope) for movement detection. Foot-worn IMUs and pressure sensors are used to determine weight, posture allocation, physical activity classification, and energy expenditure calculations, among other parameters related to the motion of the foot (gait) and/or person of the wearer. Hegde et al, developed an IMU and Force Sensing Resistor (FSR) based insole monitor named Smartstep, which can classify major postures and activities [17], energy expenditure prediction [18], estimation of the body weights (BW) [19], estimation of temporal gait parameters of healthy and post-stroke individuals [8]. A number of publications described the use of shoe-based sensor systems for various applications such as monitoring of vertical ground reaction forces [20]-[21], motion intent learning [22], plantar pressure [23]-[24], falls detection [25], estimation of the center of mass displacement during walking [26], pedestrian navigation [27] and tracking [28], and rehabilitation [29]–[33].

Attaching sensors to shoes in a reliable way is a major challenge when developing shoe-based sensor systems. To address this problem, a possible approach is to modify shoes for direct sensor integration, but it is typically labor-intensive and not feasible for large populations without the direct involvement of shoe manufacturers. Besides, modification may potentially diminish the original functionality of the shoe. Commercial sensor-equipped shoes for example, PUMA RS100 Computer Shoe [34] and Nike Lunar [35] minimized such issues. However, the durability of these products was not satisfactory due to high dynamic loads on the sensors during physical activity.

Motivated by the limitations imposed by the existing systems, the authors developed a novel wearable sensor, namely *Smart Lacelock*, that can be easily attached to a user's shoe in the form of a shoelace tensioning device without any modification of the shoe. The use of this sensor in people's daily life is largely effortless and eliminates the need for tying shoelaces or straps. Further, this sensor provides accurate information on the wearer's lower body movement. The *Smart Lacelock* incorporates an IMU to measure the spatial motion of the shoe. Additionally, it also incorporates a force sensor (load cell) to measure the tension in the shoelace. Usually, the

tension of the shoelace changes due to the change of the foot shape and the shape of the foot changes due to ankle movement and foot loading. Thus, by measuring the tension of the shoelace, this sensor can provide valuable information related to ankle movement and/or foot loading.

The advantage of this device is three-fold: 1) ensures reliable inertial sensor data by providing secure and reliable attachment of the IMU without any modification of the shoe; 2) introduces a novel shoelace tension measuring technique that not only provides rich information about foot-loading and ankle movement but also provides the unique capability to recognize the unique nature of individual gait patterns/gait signature; and 3) eliminates the use of insole-based force measuring sensors to address the durability issue.

This paper details the development of the *Smart Lacelock* along with the human subject testing aimed at characterizing the performance of the device using gait data from an eight-camera motion capture system and a force platform as reference systems. The paper is organized as follows: Section II presents the details overview of the *Smart Lacelock* design, electronics hardware and sensor interfacing. Section III presents experimental procedure, and data processing. Section IV presents the results obtained in the human experiments that characterize the performance of the *Smart Lacelock*. Section V presents a discussion of the research and finally section VI summarizes the conclusions.

II. METHODS

A. Overview of the Smart Lacelock Design

For the design of the *Smart Lacelock*, the primary goal is to provide the desired sensing and data processing/storage functions with a package at a similar size/weight as regular shoelace locks. Specifically, a miniature circuit board (with IMU embedded) and the battery must be fully encapsulated in the device, and a small-scale load cell must be embedded in the load-bearing structure for force sensing. Further, the device should have a separable structure, with two individual pieces embedded in the shoelaces on the opposite sides of the shoe. Further, the two pieces must be easy to detach and attach to facilitate the device's practical daily use.

To fulfill these requirements, a *Smart Lacelock* prototype is shown in Fig. 1. The device comprises two assemblies:

- 1) Assembly A consists of a Lace Tensioner A (#5), a Load Cell (#3), and a Female Coupler (#1), connected with 4 screws (#6) as shown in Fig. 1(a). The Lace Tensioner A (#5) has three holes to route the shoelace. In addition, an Electronics Enclosure (#9), rigidly attached to the Lace Tensioner A or Female Coupler, is also part of Assembly A. The Electronics Enclosure (#9) houses an inertia measurement unit (IMU), a load cell signal conditioning circuit, a microprocessor, a battery, and the other electronic components and circuit boards for sensor interfacing, data processing, and storage, as shown in Fig 1(b) (right).
- 2) Assembly B consists of a Lace Tensioner B (#4) rigidly attached with a Male Coupler (#2). Similar to the Lace Tensioner A (#5), the Lace Tensioner B (#4) also has three holes to route the shoelace as shown in Fig. 1(a).

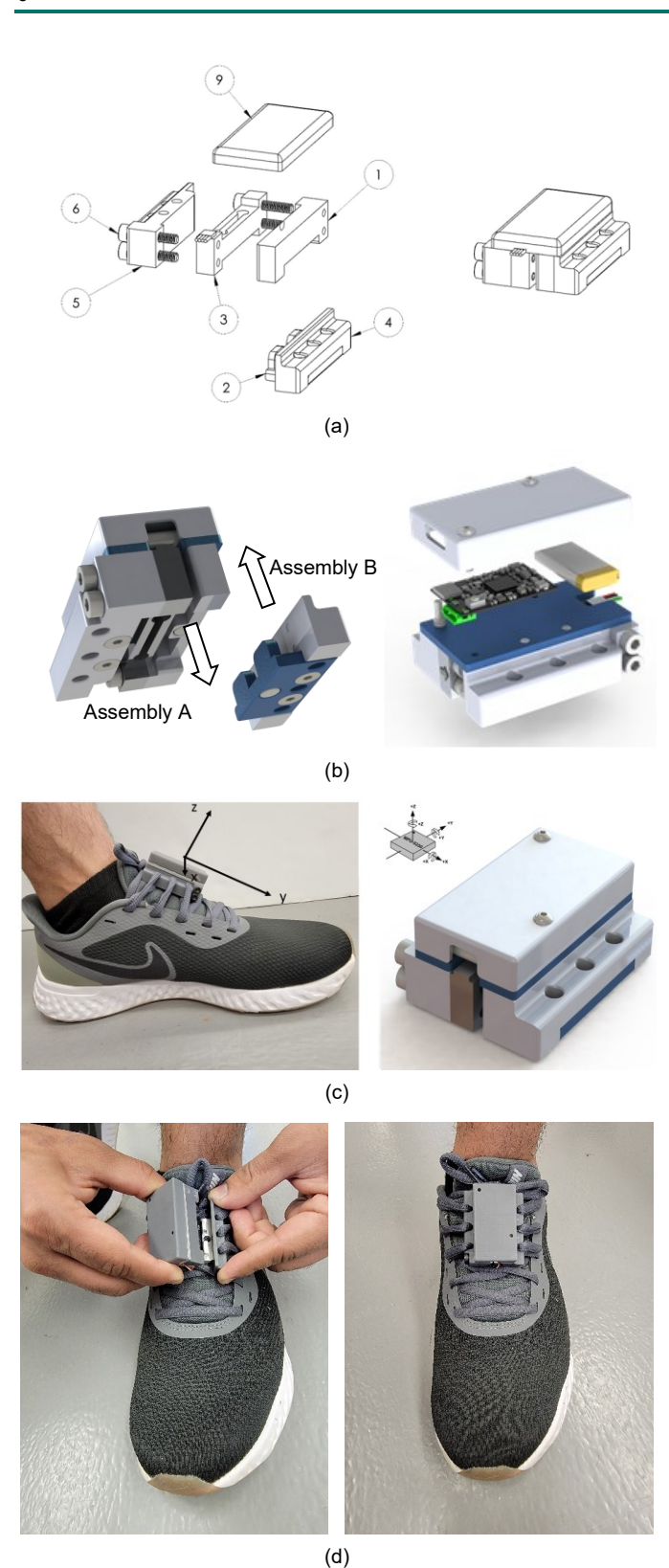


Fig. 1. (a) Shoelace sensor design (Exploded view); Components in the figures above (#1) Female Coupler, (#2) Male Coupler, (#3) Load Cell, (#4) Lace Tensioner B, (#5) Lace Tensioner A, (#6) Screws, and (#9) Electronics Enclosure; (b) Smart Lacelock locking and unlocking mechanism (left) and the Electronics Enclosure of the smart lacelock (right); (c) The smart lacelock's IMU orientation; (d) Locking and unlocking mechanism (left) and the Smart Lacelock device is in locked state ready for testing (right).

To use the *Smart Lacelock*, each assembly is attached to one side of the shoe, with the shoelace routed through the holes in the Lace Tensioners A and B (#5 and #4). Subsequently, the two assemblies are securely attached to each other by inserting the teeth of the Male Coupler (#2) into the slots in the Female Coupler (#1), as shown in Fig. 1(b) (left). For the reliability of attachment, both the Male Coupler (#2) and Female Coupler (#1) have a magnet embedded on the mating surface, such that the pulling force between the magnets ensures the assemblies to stay together in the locked state. To unlock, the Assembly A should be lifted upwards such that the teeth of the Male Coupler slide out of the slots in the Female Coupler. As such, the assemblies can be attached and detached with minimum effort from the user.

B. Electronics Hardware and Sensor Interfacing

The electronics of the *Smart Lacelock* device consist of a miniature loadcell - 500g, Straight Bar (TAL221), and a 9-DOF IMU along with data acquisition electronics powered by a 3.7 V Li-polymer battery of 100 mAh capacity. This system also incorporated STM32L476RG, a Cortex-M4 Ultra-low-power ARM processor (ST Microelectronics, Geneva, Switzerland) with an 80 MHz CPU at 39 $\mu A/MHz$; a 32 GB micro-SD card to store data sampled at 512 Hz by the microcontroller unit (MCU); and a micro-USB interface to control data collection, access sensor signals stored in the SD card, update MCU timestamp, recharge the battery, and upload the firmware. A small 4-layer PCB (32mm x 24 mm) was designed and manufactured to incorporate all electronics components of the device. The fully assembled PCB together with the battery weighs 6g.

The mini loadcell was interfaced with the MCU through HX711 (a precision 24-bit analog-to-digital converter) using the serial interface. The motion tracking was performed by the IMUs (MPU-9250, InvenSense Inc., San Jose, CA, USA), each combining a 3-axis gyroscope and a 3-axis accelerometer. The orientation of the IMU accelerometer and gyroscope is shown in Fig. 1(c). The accelerometer and gyroscope of the module were configured to have a ± 16 g and ± 2000 dps measurement range, respectively, with 16 bits of resolution. The IMU was interfaced with the MCU through SPI interface.

III. EXPERIMENTAL PROCEDURE

A. Experimental Protocol

To demonstrate the functionality and performance of the proposed *Smart Lacelock* in the measurement of human movement, we conducted a human study that involved ten healthy participants (Anthropometric Data summarized in TABLE I) with no physical and cognitive abnormalities. Participants were informed about the research procedure and signed a written consent form approved by the University of Alabama Institutional Review Board. Participants were asked to wear athletic clothing and running shoes.

Then, they were fitted with 34 reflective markers and the *Smart Lacelock*. Markers were secured on the subject skin/clothes using double-sided tape to record 3D motion with an infrared motion tracking system at a sample frequency of

TABLE I
ANTHROPOMETRIC DATA OF THE PARTICIPANTS

Subject	Gender	Age	Weight	Height	Shoe
		(year)	(kg)	(cm)	Size
					(US)
1	Male	26	84	177.8	8.5
2	Male	30	64	175.25	8.5
3	Male	26	78	172.72	10
4	Female	30	55	169	8
5	Male	26	72	1.75.25	9
6	Female	27	84	167.64	8
7	Male	32	63.5	167.64	9
8	Male	25	61	162.56	8
9	Male	25	76	170.18	8.5
10	Male	28	68.5	167.64	9

100 Hz (Vicon Nexus and Vero infra-red Cameras, UK). The *Smart Lacelock* were fitted on the participant's shoes (left and right). The two parts of the *Smart Lacelock* were separately mounted by routing the shoelace through the holes in the *Smart Lacelock* and then attached with each other through the embedded locking mechanism, as shown in Fig. 1(d). Slight adjustments were performed to make it comfortable as well as to obtain the desired level of tightness. Once the laces were adequately tensioned, the *Smart Lacelock* device was in a locked state, ready for testing. A multi-axis force platform (AccuGait OptimizedTM, AMTI, Watertown, MA, USA) embedded at the center of a walkway was to record the ground reaction force (GRF) at a sampling frequency of 1000 Hz.

Four activities were performed in random order by all participants: 1) Free ankle swing, 2) Bodyweight shifting, 3) Sit-to-stand, and 4) Overground walking. Free ankle swing and bodyweight shifting activities were chosen to understand the effect of ankle movement and foot loading on shoelace tension. Indeed, the tension of the shoelace changes due to the shape change of the foot, and the main reasons behind this change are ankle movement and foot loading. Common activities of daily living such as sit-to-stand and overground walking were also selected because: 1) they involve ankle movement and foot loading, thus the combined effect of ankle movement and foot loading on shoelace tension can be observed; and 2) they involve significantly different limb/joint movements (small-range cyclical movements during walking, and big-range, transitional movements in sit-to-stand/stand-tosit motion).

1) Free ankle swing:

Participants sat on a chair, raised one of their feet parallel to the ground, and performed at least 20 plantarflexion and 20 dorsiflexion while keeping the rest of the leg as stationary as possible. This activity was then repeated for the contralateral foot (total 80 trials).

2) Bodyweight shifting:

Participants stood beside the force plate and gradually shifted the weight on it by keeping the ankle as stationary as possible. Data were recorded for at least 10 successful weight-shifting on the force platform with the right and left feet (total of 20 trials). A trial was considered successful if the subject ankle joint movement was minimal or within a very small range (5 degrees).

3) Sit-to-stand:

Participants stood up on a force plate from a chair and then sat down on the chair. The chair was positioned very close to the force plate so that person could easily stand up on the force plate. The sit-to-stand and stand-to-sit motions were repeated 10 times (20 in total).

4) Overground walking:

Participants walked up and down the 7-m walkway. Data were recorded for at least 5 successful strikes on the force platform with the right and left feet (total of 10 trials). A trial was considered successful if the subject did not make any noticeable alterations in stride length during the trial (i.e. no targeting) and contacted the platform with the entire foot. Overground walking was repeated for self-selected slow, normal, and fast speeds in a randomized order. Familiarization trials were included in determining the optimal starting positions. Subjects could rest at any time during the experiment if they felt tired.

To observe the effect of shoes, two participants repeated the experiments using different shoes (running Vs. walking shoes).

To examine the influence of initial shoelace tension force on sensor measurement, a separate study was conducted in which a subject walked with the shoelaces tied tightly in one trial and tied loosely in the other.

Each experimental session was videotaped with an iON contour video camera at a 60fps capture rate. The Vicon system, and video camera were time-synchronized with the *Smart Lacelock* device by sending the same internet timestamp to all the devices.

B. Data Processing

Both the *Smart Lacelock* device and the eight-camera motion analysis system recorded the data simultaneously. High-frequency noise was removed from markers coordinates with a fourth-order Butterworth low-pass filter with a cut-off at 10 Hz. Markers data were used to calculate 3D ankle and knee Cardan joint angles.

During free ankle swing, the beginning of the cycle was marked when ankle angle was zero before initiating the ankle plantarflexion and the ending was marked when the ankle angle becomes zero after finishing dorsiflexion as illustrated in Fig.2.

During bodyweight shifting, the starting of the cycle was set when the vertical ground reaction force started to increase by putting the bodyweight on the force platform and the ending was marked when the vertical ground reaction force became minimum during the withdrawal of the bodyweight from the force platform as shown in Fig.3.

During sit-to-stand, the cycle started at sitting position 2 seconds before initiating the sit-to-stand transition and ended at sitting position 2 second after the stand-to-sit transition as shown in Fig.4.

During overground walking, the onset of each gait cycle was set when the anteroposterior position of the heel marker reached its maximum value with respect to the sacrum marker, as illustrated in Fig.5. Data concerning the stride initiated on the force platform was used in the analysis.

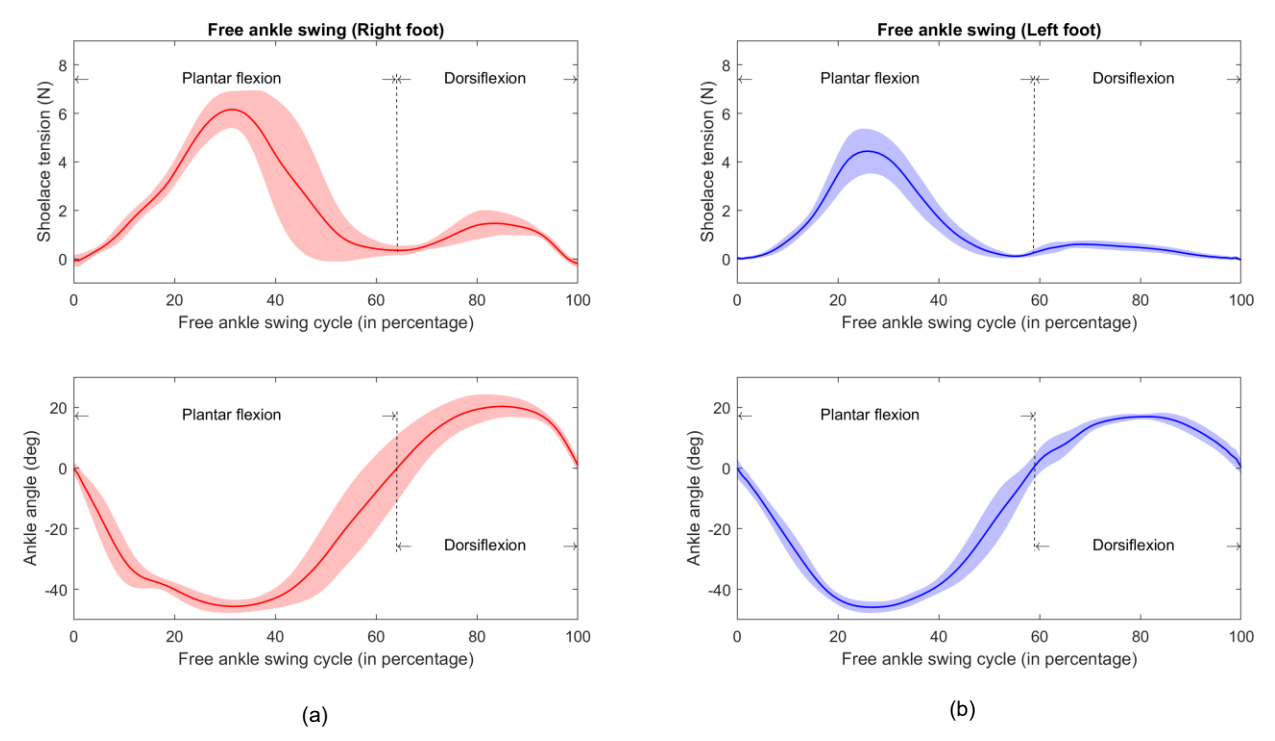


Fig. 2. Responses during free ankle swing: (a) Shoelace tension of left foot measured by Smart Lacelock (top figure) and ankle joint angle of the left foot measured by vicon motion capture system (bottom figure); (b) Shoelace tension of right foot measured by Smart Lacelock (top figure) and ankle joint angle of the right foot measured by vicon motion capture system (bottom figure).

For all movements, data in each cycle was time-interpolated over 101 points. The *Smart LaceLock* data were filtered a zero-phase lag second-order Butterworth low-pass filter with a 15 Hz cutoff frequency. The processed *Smart Lacelock* and motion camera data were averaged across all trials for each subject. The shoelace force data was calibrated to zero position (excluding the walking trials intended to evaluate the effect of initial shoelace tension force) when the foot was relaxed and flat (meaning the ankle joint angle remains zero) on the ground while sitting on a chair with no weight applied.

Finally, as an early attempt to investigate the fusion of the shoelace force and IMU sensor signals for the gait analysis purpose, the authors developed a simple Gaussian process regression model to estimate the vertical Ground Reaction Force (vGRF). The force plated-measured vGRF was used as the ground truth for model training and validation. The algorithm was developed and tested using the Statistical and Machine Learning Toolbox in MATLAB (R2020a). For each participant, approximately 67% of the data were used for the training of the regression model, while the remaining data were used for testing and performance evaluation. The results are presented in the subsequent section.

IV. RESULTS

A. Free ankle swing

Fig.2 shows the shoelace tension of both feet measured by the *Smart Lacelock* during free ankle swing, along with the respective ankle joint angle measured by the vicon motion capture system. The shoelace tension of both feet demonstrates an observable change during ankle free swing motion. Besides, the shape of the tension trajectory is

consistent over all the trials performed by the subject. A major observation from the response is that the shoelace tension increases for both plantarflexion and dorsiflexion. However, the magnitude of the increase is higher for the plantarflexion than the dorsiflexion.

B. Bodyweight shifting

Fig. 3. presents the shoelace tension (measured by *Smart Lacelock*) and vertical ground reaction force (measured by reference force plate) during the bodyweight shifting experiment. The figure shows that the shoelace tension

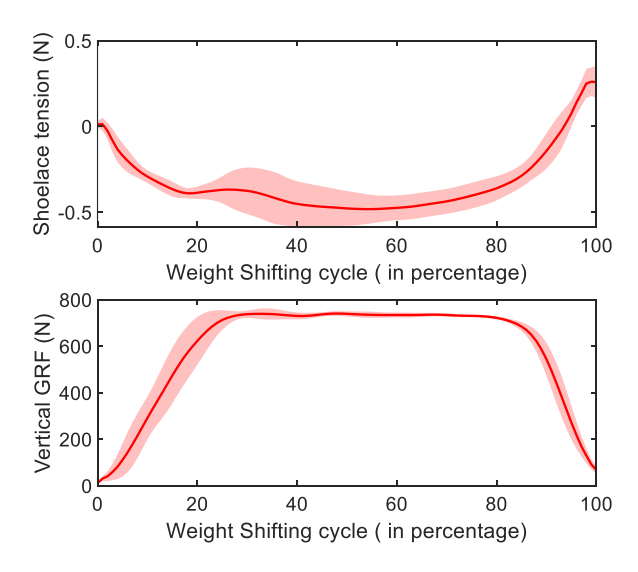


Fig. 3. Lace-lock loadcell response during body weight shifting (top figure), and Vertical ground reaction force measured from reference force platform (bottom figure).

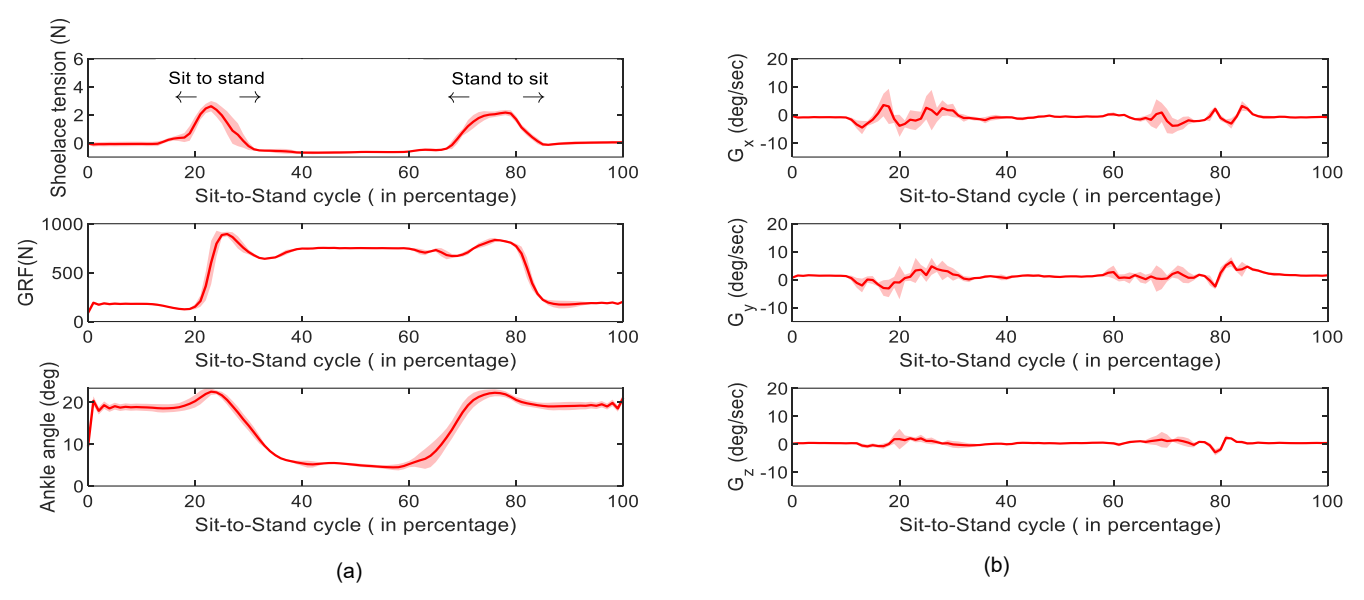


Fig. 4. The Smart Lacelock sensor outputs and the related external measurements during sit-to-stand and stand-to-sit transitions: (a) load cell-measured shoelace force (top) and the corresponding GRF (middle) and ankle angle (bottom) trajectories; (b) IMU gyroscope (Gx, Gy, Gz) signals.

reduces with respect to gradual weight shifting and becomes minimum when full body weight is applied. As mentioned earlier, the shoelace tension was calibrated to zero when the foot was flat with no weight applied; hence the negative sign does not indicate the opposite direction of the tension; instead, it means the reduction of the tension from its initial state. It is also observed that there is no significant change in the response when the person tries to stay still by applying total body weight. The shoelace tension increases when the person gradually withdraws the weight from the force plate.

C. Sit-to-stand

The results of the sit-to-stand experiment are shown in Fig. 4. Fig. 4(a) shows the shoelace tension (top figure), the

reference ground reaction force from the force platform (middle figure), and the ankle joint angle from the motion capture system (bottom figure). The figure demonstrates a specific shape of lace tension trajectory during sit-to-stand motion for all trials performed by the participants. By comparing the response with vertical ground reaction force, the loadcell response shows an early sign of the motion even before the person starts to stand up by putting weight on the force plate. Similar to sit-to-stand, stand-to-sit shows a specific shape of the lace tension trajectory. It is also observable that during the standing part of the trajectory, lace tension stays minimum which is clearly reflected by the sensor's loading condition response as described in the bodyweight shifting experiment.

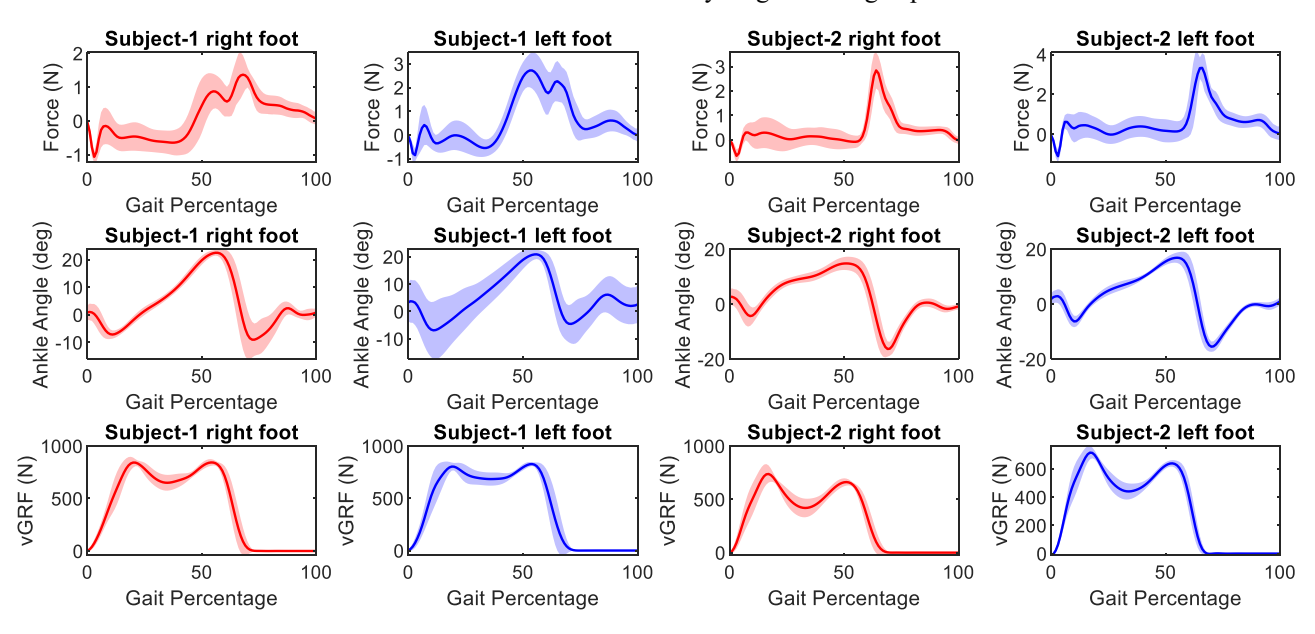


Fig. 5. Lace-lock loadcell responses during overground walking for different participants (top row); Respective ankle joint angle (middle row); and Respective vertical ground reaction force from reference force plate (bottom row).

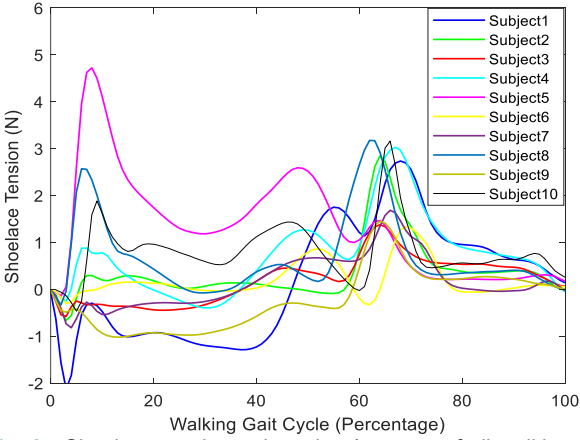


Fig. 6. Shoelace tension trajectories (average of all walking trials of each participant) for different participants during overground walking.

The Smart Lacelock's IMU gyroscope responses (Fig. 4(b)) are also compared against shoelace tension, vertical ground reaction force, and reference ankle angle during sit-to-stand and stand-to-sit motion. The figure shows that there are no distinguishable responses from the gyroscope during this activity mode.

D. Overground walking

The response of the *Smart Lacelock* device during the overground walking condition of different participants, the respective vertical ground reaction force and ankle angle trajectories are shown in Fig. 5. Fig. 5 demonstrates that the shoelace tension trajectory maintains a specific shape for each participant during walking. The shape is consistent among both feet for all trials. As illustrated in Fig.6, the shapes of thelace tension trajectories are different between participants. The shape remains the same for each person in all different trials which indicate that the *Smart Lacelock* sensor may be able to distinguish different walking profile among different participants.

In order to observe the effect of different shoes on the device, participants used different shoes to repeat the experiments. Fig. 7 shows the comparison between shoelace tension trajectory during walking while the same person was wearing two different shoes. Although the amplitudes of the trajectories are little different, but the shape remains similar

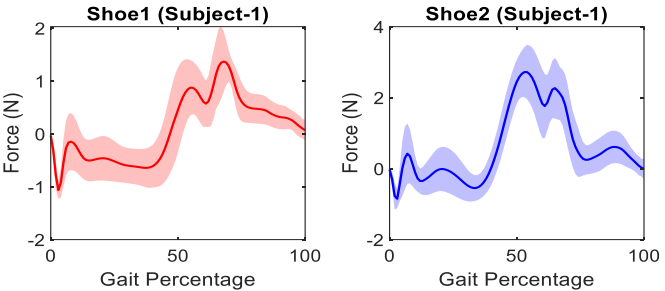


Fig. 7. Smart Lace-lock loadcell response during for same subject with different shoes during overground walking condition.

for both shoes, which further validates the *Smart Lacelock*'s ability to detect person's specific walking gait profile without any significant effect from the shoe.

The IMU of the *Smart Lacelock* device measures the overall motion of the wearer's leg and foot during the walking cycle. There have been numerous research that shows inertial sensor responses on the back of the foot. Hence, this paper focuses more on the shoelace tension trajectory. But the data collected from the IMU shows consistency among participants during different trials. The IMU accelerometer z-axis responses of different subjects during walking are shown in Fig. 8.

E. Overground walking with different initial shoelace tenisions

Fig. 9 depicts the responses of the Smart Lacelock device during overground walking with laces tied loosely versus tightly by the same participant. The result demonstrates that the shape of the shoelace tension trajectory is unaffected by initial lace tension forces. On the other hand, the average peak-to-peak range of shoelace force trajectory increases from 1.87 N at the low initial tension to 2.28 N at the high initial tension, suggesting a scaling effect associated with the initial tension. After removing the initial tension and scaling the signal based on the initial tension, the processed shoelace force trajectories display good consistency, despite the different initial tensions.

F. Estimation of vGRF during walking

Table II summarizes the performance of the vGRF estimation algorithm. The correlation coefficient and the root

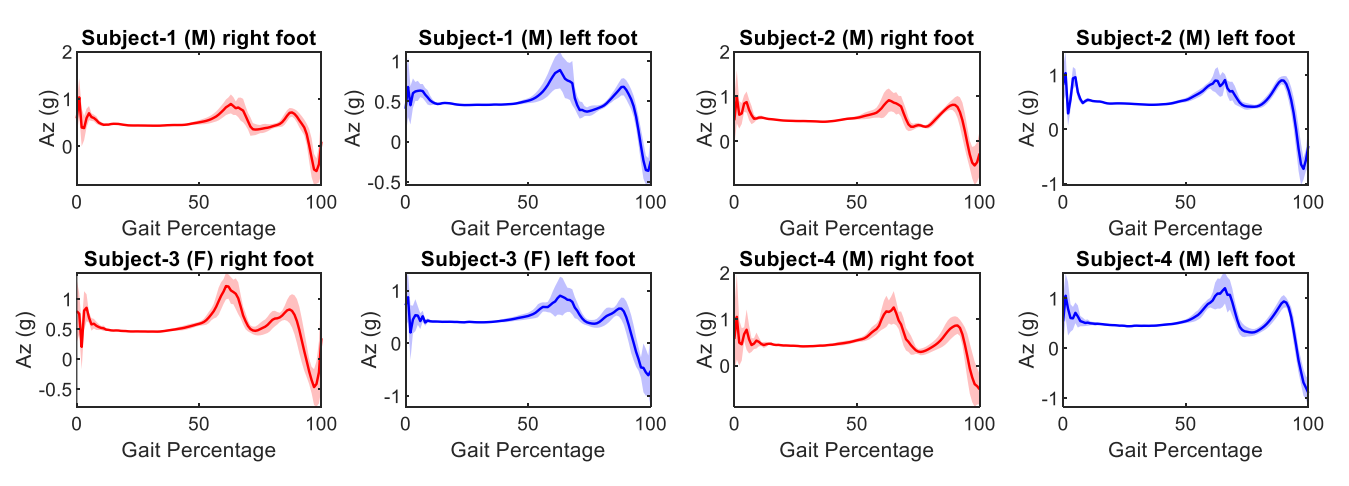


Fig. 8. Smart Lace-lock accelerometer z-axis response during overground walking of different participants.

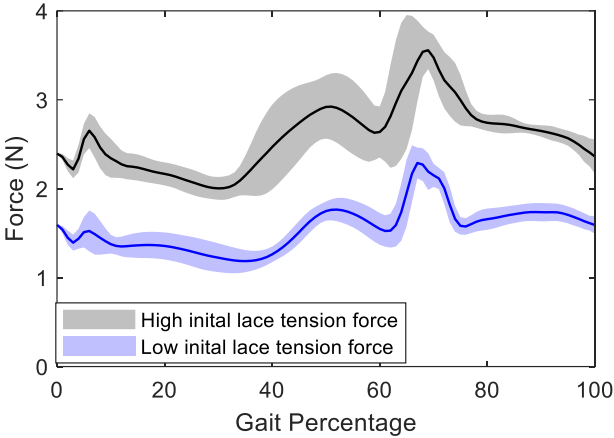


Fig. 9. Lace-lock loadcell responses during overground walking for two different initial shoelace tensions.

mean squared error (RMSE) were calculated as the performance measures. Considering the unique capability of measuring the shoelace force provided by the Smart Lacelock, the regression algorithm was developed under two conditions: with and without the shoelace force as an input, with the purpose of quantifying the contribution from the shoelace force signal. As can be observed in the table, fusing the shoelace force signal with the IMU signals clearly improves the performance (compared with IMU-only estimation). Overall, the average correlation coefficients were calculated as 0.89 (IMU-only) and 0.90 (IMU and shoelace force fusion), and the average RMSE were 0.17 body weight (BW) (IMUonly) and 0.16 BW (IMU and shoelace force fusion). The typical performance of the vGRF estimation (estimated vs estimated vGRFs) is shown in Fig. 10. Note that the regression modeling was conducted using the basic Gaussian

TABLE II
THE PERFORMANCE OF THE VGRF ESTIMATION ALGORITHM

Subject ID	Correlation coefficient		Root mean square error (BW)		
	IMU data	IMU and loadcell data	IMU data	IMU and loadcell data	
1	0.8710	0.9150	0.1689	0.1353	
2	0.9571	0.9571	0.1686	0.1497	
3	0.8519	0.8765	0.1770	0.1628	
4	0.7152	0.7783	0.2449	0.2124	
5	0.9463	0.9440	0.1195	0.1228	
6	0.8871	0.8659	0.2016	0.2172	
7	0.8433	0.8115	0.2313	0.2534	
8	0.9344	0.9600	0.1302	0.1010	
9	0.9585	0.9487	0.0933	0.1026	
10	0.9261	0.9188	0.1256	0.1267	

process regression technique. In the future, more advanced machine learning technique may be used to further improve the vGRF estimation performance.

V. DISCUSSIONS

A novel wearable *Smart Lacelock* device was designed, fabricated, and tested in this study. The device provides reliable inertial sensing through the secure and reliable attachment of an IMU to a shoe. It also incorporates a shoelace tension sensor to provide valuable information about foot-loading and ankle movement without using insole-based foot pressure measurement.

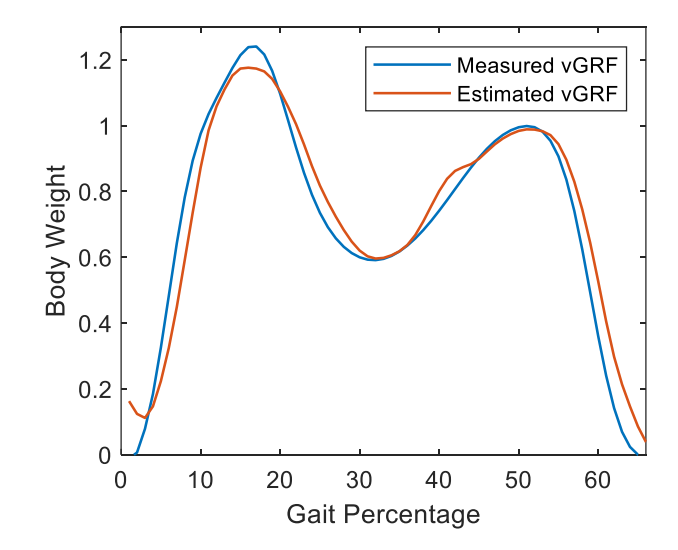


Fig. 10. Typical vGRF estimation performance (the vGRF amplitude is body weight (BW) normalized).

The free ankle swing experiment demonstrates how shoelace tension changes with ankle movement. Associated with 40° plantarflexion, the shoelace tension increases by approximately 6 N. The shoelace tension also increases during dorsiflexion. Associated with $\sim\!20^\circ$ dorsiflexion, the shoelace tension increases by 1.75 N. The difference in the shoelace tension increase (plantarflexion versus dorsiflexion), combined with the related IMU measurement, may potentially be used to estimate the ankle movement during gait analysis.

Different from free ankle swing, which increases the shoelace tension, the foot loading decreased the tension. During the body weight shifting experiment, the participant's complete body weight (about 745.56 N) causes the shoelace tension to decrease by 0.5 N as shown in Fig.3.

Results from the sit-to-stand experiments highlighted the usefulness of the shoelace force signal. The shoe-mounted IMU generates weak signals during sit-to-stand or stand-to-sit transition when the feet remain largely stationary. In contrast, the shoelace force signal demonstrated a clear shape of lace tension change during sit-to-stand motion for all trials, despite the fact that the feet remained motionless during this activity. In addition, the loadcell response revealed an early indication of the motion before the subject started to stand up by shifting the body weight to the feet, which may be exploited to identify the intent of standing-up motion. The shoelace tension trajectory also demonstrated a clear sign of loading and unloading during this activity which helped to distinguish the sitting part from the standing part.

The usefulness of the shoelace force signal also lies in its fusion with the IMU signals to support gait analysis of walking, which was demonstrated in the regression-based vGRF estimation. Compared with IMU-only estimation, the fusion of the shoelace force-IMU signals provides a relatively small but clear improvement in the performance. Additionally, from the results of overground walking experiments, two observations can be made. First, the shoelace tension trajectory maintained a specific shape (for both left and right foot) for each person during walking, which indicates the unique gait patterns of the individuals. Second,

the shape did not change if the person changed the speed or used different shoes. Hence, the *Smart Lacelock* showed great promise in identifying the unique nature of individual gait patterns or gait signatures.

Based on the results from this study, the authors envision that the Smart Lacelock may serve a variety of applications in For example, based on the quantitative measurement of walking gait, the Smart Lacelock may provide daily-life monitoring and evaluation of the gait quality of older adults and individuals with mobility impairments, and the gait information may also support the identification of increased risk of fall. Exploiting the unique patterns of shoelace force and IMU signal trajectories associated with different activities, the Smart Lacelock may enable accurate recognition of human activities and provide more accurate estimate of energy expenditure compared with existing wearable sensors. Overall, the Smart Lacelock may become a highly useful and accessible wearable sensor in the future and benefit people with detailed and real-time accessible data about their walking gait, physical mobility, and physical activities.

VI. CONCLUSIONS

This article presents the design and experimental testing of a novel wearable Smart Lacelock device. Unlike existing shoebased wearable sensors, this device can be easily attached to a user's shoe in the form of a shoelace tensioning device without any modification of the shoe. The device incorporates an embedded IMU to provide reliable measurement of the spatial motion of the foot. The force sensor of the device measures the tension in the shoelace, which provides valuable information related to the ankle movement and the foot loading, thus eliminating the needs for low-durability insolebased pressure sensor. The sit-to-stand experiment results shows that shoelace tension maintain a specific shape during this activity even when the foot remains stationary during this transition. The result also demonstrates an early sign of the motion even before the person starts to stand, which could be useful information for sit-to-stand intent recognition. The overground walking experiment validates the device's ability to recognize the unique nature of individual gait patterns. The ability to recognize individual gait patterns presents a first step towards establishing a powerful wearable device that can be used as the basis for many future applications such as gait quality monitoring, evaluation of the risk of fall, activity recognition, and energy expenditure estimation.

REFERENCES

- [1] Y. Lu and S. Velipasalar, "Autonomous Human Activity Classification From Wearable Multi-Modal Sensors," *IEEE Sensors Journal*, vol. 19, no. 23, pp. 11403–11412, Dec. 2019, doi: 10.1109/JSEN.2019.2934678.
- [2] S. Majumder and M. J. Deen, "Wearable IMU-Based System for Real-Time Monitoring of Lower-Limb Joints," *IEEE Sensors Journal*, vol. 21, no. 6, pp. 8267–8275, Mar. 2021, doi: 10.1109/JSEN.2020.3044800.
- [3] V. Bijalwan, V. B. Semwal, and T. K. Mandal, "Fusion of Multi-Sensor-Based Biomechanical Gait Analysis Using Vision and Wearable Sensor," *IEEE Sensors Journal*, vol. 21, no. 13, pp. 14213–14220, Jul. 2021, doi: 10.1109/JSEN.2021.3066473.
- [4] G. Li, T. Liu, and J. Yi, "Wearable Sensor System for Detecting Gait Parameters of Abnormal Gaits: A Feasibility Study," *IEEE Sensors*

- *Journal*, vol. 18, no. 10, pp. 4234–4241, May 2018, doi: 10.1109/JSEN.2018.2814994.
- [5] L. Wang, Y. Sun, Q. Li, and T. Liu, "Estimation of Step Length and Gait Asymmetry Using Wearable Inertial Sensors," *IEEE Sensors Journal*, vol. 18, no. 9, pp. 3844–3851, May 2018, doi: 10.1109/JSEN.2018.2815700.
- [6] A. R. Anwary, H. Yu, and M. Vassallo, "Optimal Foot Location for Placing Wearable IMU Sensors and Automatic Feature Extraction for Gait Analysis," *IEEE Sensors Journal*, vol. 18, no. 6, pp. 2555–2567, Mar. 2018, doi: 10.1109/JSEN.2017.2786587.
- [7] R. Wagner and A. Ganz, "PAGAS: Portable and Accurate Gait Analysis System," Annu Int Conf IEEE Eng Med Biol Soc, vol. 2012, pp. 280–283, 2012, doi: 10.1109/EMBC.2012.6345924.
- [8] P. Lopez-Meyer, G. D. Fulk, and E. S. Sazonov, "Automatic detection of temporal gait parameters in poststroke individuals," *IEEE Trans Inf Technol Biomed*, vol. 15, no. 4, pp. 594–601, Jul. 2011, doi: 10.1109/TITB.2011.2112773.
- [9] S. J. M. Bamberg, A. Y. Benbasat, D. M. Scarborough, D. E. Krebs, and J. A. Paradiso, "Gait Analysis Using a Shoe-Integrated Wireless Sensor System," *IEEE Transactions on Information Technology in Biomedicine*, vol. 12, no. 4, pp. 413–423, Jul. 2008, doi: 10.1109/TITB.2007.899493.
- [10] B. Mariani, M. C. Jiménez, F. Vingerhoets, and K. Aminian, "On-Shoe Wearable Sensors for Gait and Turning Assessment of Patients With Parkinson's Disease," *IEEE Transactions on Biomedical Engineering*, 2013, doi: 10.1109/TBME.2012.2227317.
- [11] S. Crea, M. Donati, S. M. M. De Rossi, C. M. Oddo, and N. Vitiello, "A Wireless Flexible Sensorized Insole for Gait Analysis," *Sensors*, vol. 14, no. 1, Art. no. 1, Jan. 2014, doi: 10.3390/s140101073.
- [12] I. P. I. Pappas, T. Keller, S. Mangold, M. R. Popovic, V. Dietz, and M. Morari, "A reliable gyroscope-based gait-phase detection sensor embedded in a shoe insole," *IEEE Sensors Journal*, vol. 4, no. 2, pp. 268–274, Apr. 2004, doi: 10.1109/JSEN.2004.823671.
- [13] K. Kong and M. Tomizuka, "A Gait Monitoring System Based on Air Pressure Sensors Embedded in a Shoe," *IEEE/ASME Transactions on Mechatronics*, vol. 14, no. 3, pp. 358–370, Jun. 2009, doi: 10.1109/TMECH.2008.2008803.
- [14] T. Liu, Y. Inoue, and K. Shibata, "Development of a wearable sensor system for quantitative gait analysis," *Measurement*, vol. 42, no. 7, pp. 978–988, Aug. 2009, doi: 10.1016/j.measurement.2009.02.002.
- [15] W. Tao, T. Liu, R. Zheng, and H. Feng, "Gait Analysis Using Wearable Sensors," *Sensors (Basel)*, vol. 12, no. 2, pp. 2255–2283, Feb. 2012, doi: 10.3390/s120202255.
- [16] G. Li, T. Liu, J. Yi, H. Wang, J. Li, and Y. Inoue, "The Lower Limbs Kinematics Analysis by Wearable Sensor Shoes," *IEEE Sensors Journal*, vol. 16, no. 8, pp. 2627–2638, Apr. 2016, doi: 10.1109/JSEN.2016.2515101.
- [17] E. S. Sazonov, G. Fulk, J. Hill, Y. Schutz, and R. Browning, "Monitoring of Posture Allocations and Activities by a Shoe-Based Wearable Sensor," *IEEE Transactions on Biomedical Engineering*, vol. 58, no. 4, pp. 983–990, Apr. 2011, doi: 10.1109/TBME.2010.2046738.
- [18] N. Sazonova, R. C. Browning, and E. Sazonov, "Accurate prediction of energy expenditure using a shoe-based activity monitor," *Med Sci Sports Exerc*, vol. 43, no. 7, pp. 1312–1321, Jul. 2011, doi: 10.1249/MSS.0b013e318206f69d.
- [19] N. A. Sazonova, R. Browning, and E. S. Sazonov, "Prediction of Bodyweight and Energy Expenditure Using Point Pressure and Foot Acceleration Measurements," *Open Biomed Eng J*, vol. 5, pp. 110– 115, Dec. 2011, doi: 10.2174/1874120701105010110.
- [20] P. H. Veltink, C. Liedtke, E. Droog, and H. van der Kooij, "Ambulatory measurement of ground reaction forces," *IEEE Transactions on Neural Systems and Rehabilitation Engineering*, vol. 13, no. 3, pp. 423–427, Sep. 2005, doi: 10.1109/TNSRE.2005.847359.
- 21] L. A. Cramer, M. A. Wimmer, P. Malloy, J. A. O'Keefe, C. B. Knowlton, and C. Ferrigno, "Validity and Reliability of the Insole3 Instrumented Shoe Insole for Ground Reaction Force Measurement during Walking and Running," *Sensors*, vol. 22, no. 6, Art. no. 6, Jan. 2022, doi: 10.3390/s22062203.
- [22] J. Yang and Y. Yin, "Novel Soft Smart Shoes for Motion Intent Learning of Lower Limbs Using LSTM With a Convolutional Autoencoder," *IEEE Sensors Journal*, vol. 21, no. 2, pp. 1906–1917, Jan. 2021, doi: 10.1109/JSEN.2020.3019053.
- [23] L. Shu, T. Hua, Y. Wang, Q. Li, D. D. Feng, and X. Tao, "In-Shoe Plantar Pressure Measurement and Analysis System Based on Fabric

- Pressure Sensing Array," *IEEE Transactions on Information Technology in Biomedicine*, vol. 14, no. 3, pp. 767–775, May 2010, doi: 10.1109/TITB.2009.2038904.
- [24] M. Abdelhady, A. J. van den Bogert, and D. Simon, "A High-Fidelity Wearable System for Measuring Lower-Limb Kinetics and Kinematics," *IEEE Sensors Journal*, vol. 19, no. 24, pp. 12482– 12493, Dec. 2019, doi: 10.1109/JSEN.2019.2940517.
- [25] O. Aziz and S. N. Robinovitch, "An Analysis of the Accuracy of Wearable Sensors for Classifying the Causes of Falls in Humans," *IEEE Transactions on Neural Systems and Rehabilitation Engineering*, vol. 19, no. 6, pp. 670–676, Dec. 2011, doi: 10.1109/TNSRE.2011.2162250.
- [26] H. M. Schepers*, E. H. F. van Asseldonk, J. H. Buurke, and P. H. Veltink, "Ambulatory Estimation of Center of Mass Displacement During Walking," *IEEE Transactions on Biomedical Engineering*, vol. 56, no. 4, pp. 1189–1195, Apr. 2009, doi: 10.1109/TBME.2008.2011059.
- [27] C. Zhou, J. Downey, D. Stancil, and T. Mukherjee, "A Low-Power Shoe-Embedded Radar for Aiding Pedestrian Inertial Navigation," *IEEE Transactions on Microwave Theory and Techniques*, vol. 58, no. 10, pp. 2521–2528, Oct. 2010, doi: 10.1109/TMTT.2010.2063810.
- [28] E. Foxlin, "Pedestrian tracking with shoe-mounted inertial sensors," IEEE Computer Graphics and Applications, vol. 25, no. 6, pp. 38–46, Nov. 2005, doi: 10.1109/MCG.2005.140.
- [29] K. N. Winfree, I. Pretzer-Aboff, D. Hilgart, R. Aggarwal, M. Behari, and S. Agrawal, "An untethered shoe with vibratory feedback for improving gait of Parkinson's Patients: The PDShoe," in 2012 Annual International Conference of the IEEE Engineering in Medicine and Biology Society, Aug. 2012, pp. 1202–1205. doi: 10.1109/EMBC.2012.6346152.
- [30] C. B. Redd and S. J. M. Bamberg, "A Wireless Sensory Feedback Device for Real-Time Gait Feedback and Training," *IEEE/ASME Transactions on Mechatronics*, vol. 17, no. 3, pp. 425–433, Jun. 2012, doi: 10.1109/TMECH.2012.2189014.
- [31] C. Mancinelli et al., "A novel sensorized shoe system to classify gait severity in children with cerebral palsy," in 2012 Annual International Conference of the IEEE Engineering in Medicine and Biology Society, Aug. 2012, pp. 5010–5013. doi: 10.1109/EMBC.2012.6347118.
- [32] G. D. Fulk and E. Sazonov, "Using Sensors to Measure Activity in People with Stroke," *Topics in Stroke Rehabilitation*, vol. 18, no. 6, pp. 746–757, Nov. 2011, doi: 10.1310/tsr1806-746.
- [33] G. D. Fulk, S. R. Edgar, R. Bierwirth, P. Hart, P. Lopez-Meyer, and E. Sazonov, "Identifying Activity Levels and Steps in People with Stroke using a Novel Shoe-Based Sensor," *J Neurol Phys Ther*, vol. 36, no. 2, pp. 100–107, Jun. 2012, doi: 10.1097/NPT.0b013e318256370c.
 [34] "DigiBarn Weird Stuff: Puma RS Computer Tennis Shoes
- [34] "DigiBarn Weird Stuff: Puma RS Computer Tennis Shoes (pedometer, 1980s)." https://www.digibarn.com/collections/weirdstuff/computer-tennisshoes/ (accessed Nov. 10, 2021).
- [35] V. L. Houston, G. Luo, C. P. Mason, M. Mussman, M. Garbarini, and A. C. Beattie, "Changes in Male Foot Shape and Size with Weightbearing," *Journal of the American Podiatric Medical Association*, vol. 96, no. 4, pp. 330–343, Jul. 2006, doi: 10.7547/0960330.



Md Rejwanul Haque received his B.Sc. degree in Aeronautical engineering (AE) from Military Institute of Science and Technology (MIST), Dhaka 1216, Bangladesh. Currently, he is doing his Ph.D. in the department of mechanical engineering at The University of Alabama, Tuscaloosa, USA. Before this, he was a Lecturer in the AE department Military Institute of Science and Technology (MIST), Dhaka, Bangladesh. His research interests include advanced sensing, motion control,

wearable robotics, and intent recognition of robotic lower-limb prostheses and exoskeletons.



Md. Rafi Islam received his B.Sc. degree in Electrical and Electronic Engineering (EEE) from Chittagong University of Engineering and Technology (CUET), Bangladesh. Currently, he is doing his Ph.D. in the department of Electrical and Computer Engineering at The University of Alabama, Tuscaloosa, USA. Before this, he was a Lecturer in the Department of Electrical and Electronic Engineering Premier University, Chittagong, Bangladesh.



Zahra Bassiri received her B.A. degree in Kinesiology (KINS) and her M.A. degree in Biomechanics of Sport from University of Mazandaran (UMZ), Babolsar, Iran. Currently, she is doing her Ph.D. in the department of mechanical engineering at The University of Alabama, Tuscaloosa, USA. Her research interests lie in the areas of biomechanics, motion control, rehabilitation robotics and human movement analysis.



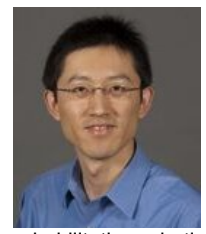
Dario Martelli joined the faculty of mechanical engineering at The University of Alabama in August 2019 as an assistant professor. Prior, he was a postdoctoral research scientist at the department of mechanical engineering of Columbia University and member of the Robotics and Rehabilitation Laboratory, where he has been since 2015. He completed his bachelor's and master's degrees in biomedical

engineering at University of Pisa, Italy, and his doctorate degree in biorobotics at Sant'Anna School of Advanced Studies, Italy. His research interests lie in the areas of rehabilitation robotics, biomechanics, and human movement analysis. Much of his work has been aimed at developing methods and technologies useful for restoration of motor functions with particular interest in the development of innovative solutions targeted at improving gait and reducing the risk of falling in patients with balance disorders. The achievement of this goal has been based on a deep understanding of how people maintain balance while walking and while reacting to unpredictable balance perturbations. His research is based on the observation that it is possible to use neuroscientific methodologies, mechatronic devices, virtual platforms, and wearable technologies to: (i) identify people at higher risk for falling; (ii) advance innovative balance and cognitive training strategies; and (iii) develop technologies able to augment balance control.



Edward Sazonov Edward Sazonov (IEEE M'02, SM'11) received the Diploma of Systems Engineer from Khabarovsk State University of Technology, Russia, in 1993 and the Ph.D. degree in Computer Engineering from West Virginia University, Morgantown, WV, in 2002. Currently he is a James R. Cudworth endowed Professor in the Department of Electrical and Computer Engineering at the University of

Alabama, Tuscaloosa, AL and the head of the Computer Laboratory of Ambient and Wearable Systems (http://claws.eng.ua.edu). His research interests span wearable devices, sensor-based behavioral informatics and methods of biomedical signal processing and pattern recognition. Devices developed in his laboratory include a wearable sensor for objective detection and characterization of food intake (AIM - Automatic Ingestion Monitor); a highly accurate physical activity and gait monitor integrated into a shoe insole (SmartStep, winner of Bluetooth Innovation WorldCup 2009); a wearable sensor system for monitoring of cigarette smoking (PACT); and others. The research in his lab was recognized by several awards, including best paper awards, President's research award at the University of Alabama and others. In 2020 Dr. Sazonov served as a Fulbright Distinguished Chair at the University of Newcastle, Australia. His research has been supported by the National Institutes of Health, National Science Foundation, National Academies of Science, as well as by state agencies, private industry and foundations. Dr. Sazonov serves as an Specialty Chief Editor for Wearable Electronics, Frontiers In Electronics and Associate Editor for several IEEE journals.



Xiangrong Shen is a professor in the department of mechanical engineering at The University of Alabama, where he has been a faculty member since 2008. He received his doctorate in mechanical engineering from Vanderbilt University in 2006, and subsequently completed a two-year postdoctoral training in rehabilitation robotics, also at Vanderbilt. Dr. Shen's research is focused on assistive and

rehabilitation robotics, and the specific topics include robotic lower-limb prostheses, portable power-assist lower-limb orthoses, and legged/wheeled robotic platforms for assistive and therapeutic purposes. His research has been supported by multiple NSF and NIH grants, including an NSF CAREER award in 2014. He served as an associate editor for the journal of Control Engineering Practice from 2008 to 2014, and currently, he serves as the chair of the ME Dynamic Systems and Control (DSC) Group and a Fellow of the Alabama Life Research Institute (ALRI).